

High-Energy Spin Dynamics in $\text{La}_{1.69}\text{Sr}_{0.31}\text{NiO}_4$

P. Bourges¹, Y. Sidis¹, M. Braden¹, K. Nakajima², and J.M. Tranquada³

¹ *Laboratoire Léon Brillouin, CEA-CNRS, CE-Saclay, 91191 Gif sur Yvette, France*

² *Neutron Scattering laboratory, ISSP, University of Tokyo, Tokai, Ibaraki, Japan*

³ *Physics Department, Brookhaven National Laboratory, Upton, NY 11973, USA*

(November 11, 2018)

We have mapped out the spin dynamics in a stripe-ordered nickelate, $\text{La}_{2-x}\text{Sr}_x\text{NiO}_4$ with $x \simeq 0.31$, using inelastic neutron scattering. We observe spin-wave excitations up to 80 meV emerging from the incommensurate magnetic peaks with an almost isotropic spin-velocity: $\hbar c_s \sim 0.32$ eV Å, very similar to the velocity in the undoped, insulating parent compound, La_2NiO_4 . We also discuss the similarities and differences of the inferred spin-excitation spectrum with those reported in superconducting high- T_c cuprates.

Magnetism plays an important role in several theories of the high-temperature superconductivity found in layered cuprates; hence, experimental characterizations of magnetic excitations in these materials have been of considerable interest. Much attention has been focussed on the “resonance” peak observed by inelastic neutron scattering in a number of different cuprates [1]. The resonance peak is centered commensurately on the antiferromagnetic wave vector. Studies of $\text{YBa}_2\text{Cu}_3\text{O}_{6+x}$, in which the resonance peak was first observed [2], have also found incommensurate excitations at somewhat lower energies [3,4]. In more recent work [5], it was found that the incommensurate scattering actually disperses downward continuously from the commensurate resonance peak, defining a single dispersive excitation.

There are several theoretical perspectives on the resonance peak and the dispersive excitations. In one popular approach, the magnetic resonance is a particle-hole bound state below the two-particle continuum associated with the d -wave superconducting gap [6–9]; such calculations, based on a homogeneous, renormalized Fermi-liquid model, yield qualitative agreement with experiment. One alternative is based on the “stripe” scenario [10,11], in which magnetic excitations are dominantly attributed to spatially segregated domains of antiferromagnetically correlated copper spins [12–16]. In particular, Batista, Ortiz, and Balatsky [17] have explicitly proposed that the dispersive resonance represents the magnon-like excitations emanating from incommensurate wave vectors associated with a stripe-correlated spin system. Their prediction that a similar resonance-like excitation should be observable in a stripe-ordered compound such as $\text{La}_{2-x}\text{Sr}_x\text{NiO}_4$ motivated the present investigation.

Regardless of whether $\text{La}_{2-x}\text{Sr}_x\text{NiO}_4$ is an ideal model for the cuprates, studies of the full spin dynamics of the incommensurate spin state are of interest, as only low-energy characterizations have been reported previously [18,19]. Here we report measurements of the high-energy spin excitations in a crystal with $x \simeq 0.31$, close to the 1/3 composition. Within the two-dimensional reciprocal

space corresponding to a doped NiO_2 plane, the diagonal stripe order yields two pairs of magnetic ordering wave vectors, $\mathbf{Q}_\delta = (\frac{1}{2}, \frac{1}{2}) \pm (\delta, \delta)$ and $(\frac{1}{2}, \frac{1}{2}) \pm (\delta, -\delta)$, due to twinning of the stripe domains. [We express wave vectors in units of the reciprocal lattice, $(2\pi/a, 2\pi/a)$, with $a = 3.82$ Å.] These incommensurate points are displaced about the antiferromagnetic propagation wave vector, $\mathbf{Q}_{\text{AF}} = (\frac{1}{2}, \frac{1}{2})$, of the undoped parent compound. The incommensurability δ varies with the hole concentration as $\delta \approx x/2$ [20], with $\delta = 0.158$ for our sample at low temperature. We observed spin-wave excitations dispersing from each \mathbf{Q}_δ peak up to a maximum of 80 meV at \mathbf{Q}_{AF} . Surprisingly, the effective spin-wave velocity, $\hbar c_s \sim 0.32$ eV Å, is almost as large as that of undoped insulating La_2NiO_4 , where $\hbar c_0 = 0.34$ eV Å [21]. Furthermore, the anisotropy in the spin-wave velocity between the directions parallel and perpendicular to the stripes is less than 15%. On warming to above the charge-ordering temperature, the excitation at \mathbf{Q}_{AF} softens somewhat, but remains well-defined.

Our single-crystal sample, grown by the floating-zone method, was the subject of a previous neutron scattering experiment [22]. The present inelastic-neutron-scattering measurements were performed on the 1T and 2T triple-axis spectrometers at the Orphée reactor of the Laboratoire Léon Brillouin in Saclay, France. Each spectrometer is equipped with Cu (111) and pyrolytic graphite (PG) monochromators and a PG (002) analyzer. Different final neutron energies of the analyzer, $E_f = 14.7, 30.5$ and 41 meV, were used in order to cover the full energy range of the magnetic spectrum. A PG filter was placed after the sample to minimize neutrons at higher-harmonic wavelengths. Most of the measurements have been performed within the $(HK0)$ scattering plane, with some data collected in the (HHL) zone.

In scanning across the \mathbf{Q}_δ peak positions at constant energy transfer, as indicated in the upper panel of Fig. 1, we expect, at low temperatures (below the spin-ordering temperature of 160 K), to pass through two spin-wave branches, corresponding to counter-propagating excita-

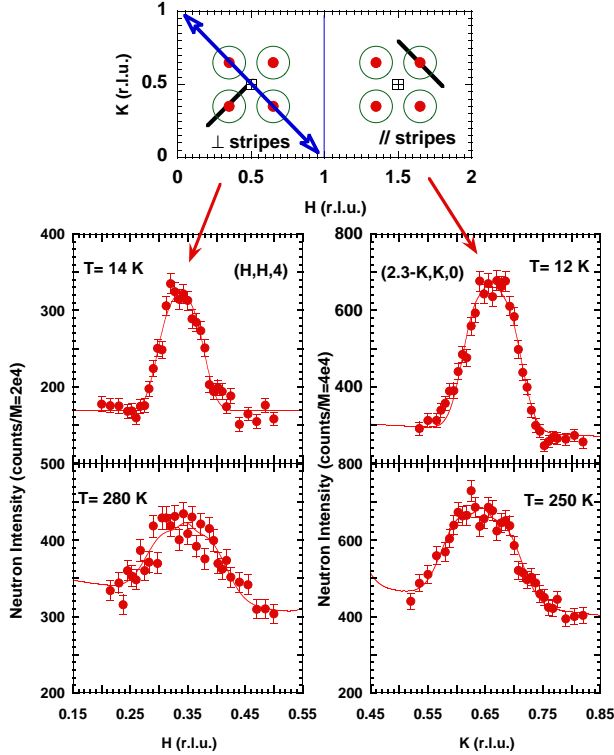


FIG. 1. upper panel) Sketch of the Brillouin zone in the reciprocal $(HK0)$ -plane. Full red circles indicate the location of the incommensurate magnetic peaks, \mathbf{Q}_δ . The green circles show the cut of the spin-waves cones at a constant energy, defining Q_ω ($\equiv \omega/c_s$ in the low-energy regime). Black bars represent the directions of the scans shown in the lower panel, the blue arrow shows the direction of the scans shown in Fig. 2. lower panels) Constant energy scans at $E = 28.1$ meV (measured with $E_f = 14.7$ meV) at two temperatures along the two directions sketched in the upper panel, probing fluctuations along wave vectors perpendicular (left) and parallel (right) to the stripes. Lines represent best fits of the extended Gaussian model described in the text.

tions. The lower panels show scans at an energy transfer of 28.1 meV along orthogonal directions with respect to the modulation wave vector. Although the two branches are not resolved, the Q -width in each case is significantly broader than resolution, with little dependence on scan direction. At higher energies [Fig. 2(b)-(d)], we clearly resolved spin waves emerging from the two \mathbf{Q}_δ points $(1.5 - \delta, 1.5 + \delta)$ and $(1.5 + \delta, 1.5 - \delta)$. At $E = 75$ meV, the excitations from $+\delta$ and $-\delta$ begin to merge at \mathbf{Q}_{AF} , forming a single broad peak, with additional weight coming from excitations associated with the orthogonal stripe domains (see Fig. 1).

The excitation at \mathbf{Q}_{AF} is better characterized by scanning the energy transfer at fixed momentum transfer. Figure 3(b)-(d) shows energy scans at \mathbf{Q}_{AF} for 3 different temperatures. The maximum of the spin excitation spectrum is $\omega_0 = 80 \pm 0.8$ meV at low temperature [Fig. 3(b)].

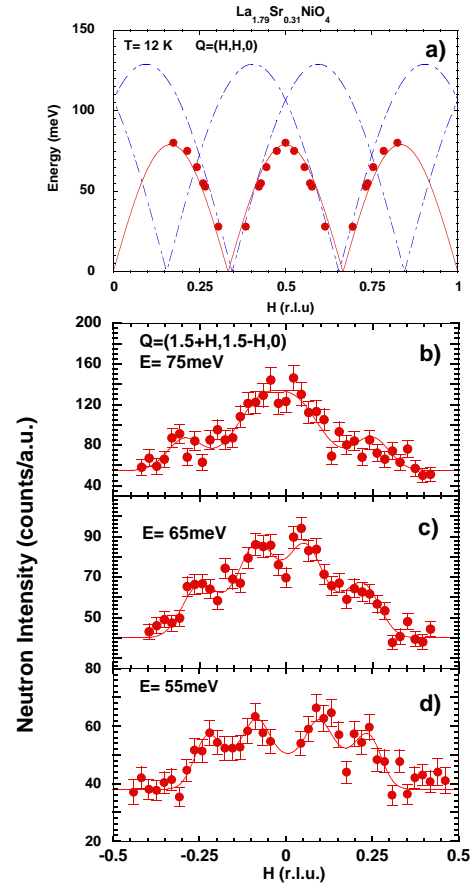


FIG. 2. Upper panel) Dispersion relation of the spin excitations in $\text{La}_{1.69}\text{Sr}_{0.31}\text{NiO}_4$. The full red line is a fit by a simple $|\sin(3\pi H)|$ function. The two blue dashed lines correspond to the spin-wave dispersion relation in undoped La_2NiO_4 , but shifted to the incommensurate wave vectors. Lower panels) Constant energy scans at b) $E = 75$ meV, c) $E = 65$ meV and d) $E = 55$ meV along $(H, -H, 0)$ (i.e., perpendicular to the stripes) around $\mathbf{Q} = (1.5, 1.5, 0)$. (b) was measured with $E_f = 41$ meV (as in Fig. 3), while (c) and (d) were measured with $E_f = 30.5$ meV. Full lines represent best fits of the extended Gaussian model described in the text.

In the studies of low-energy excitations in stripe-correlated nickelates [18,19], it was found that the observed Q -widths of the excitation peaks are broader than the energy resolution. For Sr-doped samples, this is due, at least in part, to the finite spin-spin correlation length in the ordered state. Fluctuations of the charge stripes might also play a role. To extract the frequency dispersion from the constant-energy scans of Figs. 1 and 2, we have assumed a scattering function of the form

$$S(\mathbf{Q}, \omega) = A f^2(Q) \sum_{\text{domains}} \sum_{\delta} e^{-[(\mathbf{Q} - \mathbf{Q}_\delta)^2 - Q_\omega^2]/2\Delta^2}, \quad (1)$$

where A is a scale factor, one sum is over the two incommensurate wave vectors, the other one is over the twined stripe domains, and the magnetic form factor $f(Q)$ is assumed to vary insignificantly across the range of a given

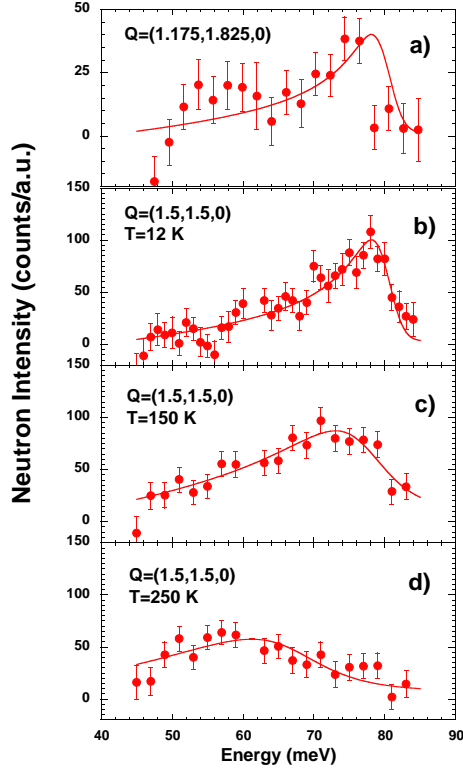


FIG. 3. Energy scans at (a) $\mathbf{Q} = (1.175, 1.825, 0)$, (b)-(d) $\mathbf{Q} = (1.5, 1.5, 0) \equiv \mathbf{Q}_{\text{AF}}$, after subtraction of background measured either at $\mathbf{Q} = (1, 2, 0)$ or by rocking the sample by $\pm 15^\circ$. The data have been obtained with $E_f = 41$ meV. The full lines represent best fits of a damped harmonic oscillator function, with a dispersion relation as shown in Fig. 2(a), convolved with the spectrometer resolution. The line in (a) is the same as in (b) except for a scale factor.

scan. To fit the data, the model $S(\mathbf{Q}, \omega)$ was convolved with the spectrometer resolution function, and the parameters Q_ω and Δ were varied to minimize χ^2 . The model provides reasonable fits to the data; note that the enhanced intensity near \mathbf{Q}_{AF} in Fig. 2(b) and (c) comes from the superposition of contributions dispersing from the four surrounding \mathbf{Q}_δ points (see the upper panel of Fig. 1). The results obtained for Q_ω as a function of energy transfer, $\hbar\omega$, are plotted in Fig. 2(a). The momentum width, Δ , when converted to half-width-at-half-maximum, is 0.05 \AA^{-1} .

To fit the constant- \mathbf{Q} scans of Fig. 3, it is standard to use an alternative parametrization:

$$S(\mathbf{Q}, \omega) = A' f^2(Q) \frac{\omega \Gamma [1 + n(\omega, T)]}{[\omega^2 - \omega^2(\mathbf{Q})]^2 + \omega^2 \Gamma^2}, \quad (2)$$

where $\omega(\mathbf{Q}) = \omega_0 - \alpha(\mathbf{Q} - \mathbf{Q}_{\text{AF}})^2$ ($\alpha = 170 \text{ meV \AA}^2$), and $n(\omega, T)$ is the Bose temperature factor. The temperature-dependence of the parameters ω_0 and Γ are plotted in Fig. 4, while the low-temperature result for ω_0 is plotted in Fig. 2(a).

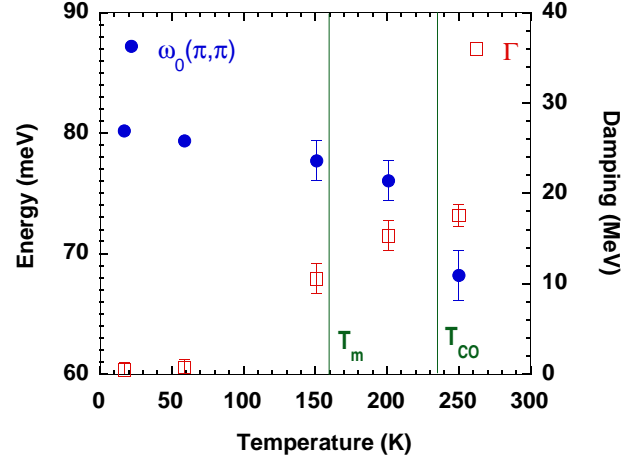


FIG. 4. Temperature dependence of various fitting parameters: Spin-wave energy maximum (left scale) and damping energy at \mathbf{Q}_{AF} (right scale). Vertical lines indicate the magnetic and charge-order transitions.

The spin-wave dispersion determined by the quantitative analysis can be described fairly well by a very simple expression: $\omega(\mathbf{Q}) = \omega_0 |\sin(3\pi H)|$ along the $[HH0]$ direction, indicated by the full line in Fig. 2(a). For comparison, the spin excitation spectrum measured in undoped La_2NiO_4 [21], shifted from \mathbf{Q}_{AF} to \mathbf{Q}_δ is indicated by dot-dashed lines. It matches the low-energy behavior surprisingly well, but clearly deviates at high energy. The \mathbf{Q}_{AF} crossing of the shifted curves is at 106 meV, while the measured ω_0 is renormalized down to 80 meV. Besides the maximum at $H = \frac{1}{2}$, the model dispersion curve also has maxima at $H = \pm \frac{1}{6}$. The energy scan in Fig. 3(a) shows that the observed maximum energy at $H \approx \frac{1}{6}$ is essentially the same as that at \mathbf{Q}_{AF} , and that the structure factors are similar as well. Looking at Fig. 2(a), one might expect to find an additional optical spin-wave branch at higher energies ($\lesssim 125$ meV); searches at energies of up to 100 meV did not yield any positive evidence for such a branch.

It is interesting to compare the doping dependence of the maximum spin-excitation frequency, ω_0 , with that of the “2-magnon frequency”, $\nu_{2\text{mag}}$, determined by Raman scattering [23–25]. We find that the ratio $\omega_0(x = 0.31)/\omega_0(x = 0) = 80 \text{ meV}/124 \text{ meV} = 0.65$ is very similar to $\nu_{2\text{mag}}(x = 0.33)/\nu_{2\text{mag}}(x = 0) = 1110 \text{ cm}^{-1}/1640 \text{ cm}^{-1} = 0.68$. In the Raman studies of the $x = 0.33$ phase [23,24], a second, lower-energy peak at 720 cm^{-1} ($\equiv 90 \text{ meV}$) was also attributed to 2-magnon scattering; however, we do not observe any features in the single-magnon dispersion that would correlate with a second 2-magnon peak. Alternatively, a Raman study of oxygen-doped La_2NiO_4 [25] suggests that the 720 cm^{-1} feature might be associated with a phonon mode, observed even in undoped La_2NiO_4 , that should be Raman

inactive.

To evaluate the anisotropy in the dispersion, we return to the 28-meV data of Fig. 1. By fitting the resolution-convolved Eq. (1) to the low temperature data, we can estimate the spin wave velocity, $c_s = \omega/Q_\omega$, along directions parallel and perpendicular to the stripes. Consistent with the figure, we find little anisotropy, with $\hbar c_{s\parallel} = 300 \pm 20$ meV Å and $\hbar c_{s\perp} = 350 \pm 20$ meV Å. Both of these values are close to the value of $\hbar c_0 = 340$ meV Å obtained in pure La_2NiO_4 [21]. The lack of significant anisotropy is rather counter-intuitive. The observation of well-defined excitations following a simple dispersion curve such as shown in Fig. 2(a) is rather remarkable relative to the large hole concentration. One can suggest that charge order coherently affects the spin dynamics for this hole filling near $\frac{1}{3}$ due to pinning effects.

As shown by Figs. 1 and 3, a striking temperature dependence is observed at energies much larger than the temperature. With increasing temperature, the magnetic mode at \mathbf{Q}_{AF} softens and broadens upon heating, starting near the magnetic ordering temperature, T_m (Fig. 4). The frequency reduction and damping are of comparable magnitude. It is of particular interest that the mode remains underdamped above the charge-ordering transition. This observation is consistent with the stripe-liquid phase proposed to describe the low-energy spin dynamics [19].

Returning to our original motivation [17], the spin excitation spectrum in our stripe-ordered nickelate does have a straightforward similarity to that measured in the superconducting state of cuprates [5]. In both cases, a downward dispersion is observed below a maximum frequency at the AF wave vector. Of course, there are also clear differences: in particular, the spin excitation spectrum of the nickelate is not limited to only a small portion of reciprocal space around \mathbf{Q}_{AF} . We observe symmetric dispersions and structure factors about the incommensurate wavevectors. These results compare somewhat better with the excitations observed in $\text{La}_{2-x}\text{Sr}_x\text{CuO}_4$, where low energy incommensurate peaks appear to merge into a broad commensurate response around ~ 25 meV [26,27]; however, in the latter case the merging occurs at a much lower energy than the value one would deduce from the cuprate spin-wave velocity and the incommensurability. In any case, the canonical nature of the ordered stripes in the nickelate limits the degree to which a direct comparison with the cuprates is practical. A more relevant point for comparison may be the high-temperature phase of the nickelate where, in the absence of static magnetic or charge order, the high-energy spin excitations remain underdamped.

In conclusion, we have measured the complete spin excitation spectrum in the stripe-ordered nickelate $\text{La}_{1.69}\text{Sr}_{0.31}\text{NiO}_4$. The deduced spin-wave velocity is surprisingly large, and there is remarkably little anisotropy between directions parallel and perpendicular to the

stripes. This spin dynamics study, in comparison with those reported for superconducting cuprates, should help to clarify the role and relevance of stripes in oxides.

We wish to thank A.V. Balatsky, C. Morais-Smith, and J. Zaanen for fruitful discussions. Work at Brookhaven is supported by U.S. Department of Energy Contract No. DE-AC02-98CH10886. Work at ISSP is supported by a Grant-In Aid for Scientific Research from the Ministry of Education, Culture, Sports, Science, and Technology, Japan

-
- [1] H. He *et al.*, *Science* **295**, 1045 (2002).
 - [2] P. Bourges, in *The Gap Symmetry and Fluctuations in High Temperature Superconductors*, edited by J. Bok, G. Deutscher, D. Pavuna, and S. A. Wolf (Plenum, New York, 1998), p. 349 (cond-mat/9901333).
 - [3] H. A. Mook *et al.*, *Nature* **395**, 580 (1998).
 - [4] M. Arai *et al.*, *Phys. Rev. Lett.* **83**, 608 (1999).
 - [5] P. Bourges *et al.*, *Science* **288**, 1234 (2000).
 - [6] F. Onufrieva and P. Pfeuty, *Phys. Rev. B* **65**, 054515 (2002).
 - [7] M. R. Norman, *Phys. Rev. B* **63**, 092509 (2001).
 - [8] A. V. Chubukov, B. Jankó, and O. Tchernyshyov, *Phys. Rev. B* **63**, 180507R (2001).
 - [9] J. Brinckmann and P. A. Lee, *Phys. Rev. B* **65**, 014502 (2001).
 - [10] V. J. Emery, S. A. Kivelson, and J. M. Tranquada, *Proc. Natl. Acad. Sci. USA* **96**, 8814 (1999).
 - [11] J. Zaanen, *Science* **286**, 251 (1999).
 - [12] J. Zaanen, M. L. Horbach, and W. van Saarloos, *Phys. Rev. B* **53**, 8671 (1996).
 - [13] N. Hasselmann, A. H. Castro Neto, C. Morais Smith, and Y. Dimashko, *Phys. Rev. Lett.* **82**, 2135 (1999).
 - [14] S. Sachdev, *Science* **288**, 475 (2000).
 - [15] E. Kaneshita, M. Ichioka, and K. Machida, *J. Phys. Soc. Jpn.* **70**, 866 (2001).
 - [16] S. Varlamov and G. Seibold, *Phys. Rev. B* **65**, 075109 (2002).
 - [17] C. D. Batista, G. Ortiz, and A. V. Balatsky, *Phys. Rev. B* **64**, 172508 (2001).
 - [18] J. M. Tranquada, P. Wochner, and D. J. Buttrey, *Phys. Rev. Lett.* **79**, 2133 (1997).
 - [19] S.-H. Lee *et al.*, *Phys. Rev. Lett.* **88**, 126401 (2002).
 - [20] H. Yoshizawa *et al.*, *Phys. Rev. B* **61**, R854 (2000).
 - [21] K. Nakajima *et al.*, *J. Phys. Soc. Jpn.* **62**, 4438 (1993).
 - [22] J. M. Tranquada *et al.*, *Phys. Rev. Lett.* **88**, 075505 (2002).
 - [23] G. Blumberg, M. V. Klein, and S.-W. Cheong, *Phys. Rev. Lett.* **80**, 564 (1998).
 - [24] K. Yamamoto, T. Katsufuji, T. Tanabe, and Y. Tokura, *Phys. Rev. Lett.* **80**, 1493 (1998).
 - [25] S. Sugai, N. Kitamori, S. Hosoya, and K. Yamada, *J. Phys. Soc. Jpn.* **67**, 2992 (1998).
 - [26] S. Petit *et al.*, *Physica B* **234-236**, 800 (1997).
 - [27] M. Matsuda *et al.*, *Phys. Rev. B* **49**, 6958 (1994).